Downloaded from http://jgs.lyellcollection.org/ at University College Dublin on April 29, 2014

Journal of the Geological Society Online First

Brittle structures focused on subtle crustal heterogeneities: implications for flow in fractured rocks

A. M. Soden, Z. K. Shipton, R. J. Lunn, S. I. Pytharouli, J. D. Kirkpatrick, A. F. Do Nascimento and F. H. R. Bezerra

Journal of the Geological Society, first published April 28, 2014; doi 10.1144/jgs2013-051

Email alerting service	click here to receive free e-mail alerts when new articles cite this article
Permission request	click here to seek permission to re-use all or part of this article
Subscribe	click here to subscribe to Journal of the Geological Society or the Lyell Collection
How to cite	click here for further information about Online First and how to cite articles

Notes

© The Geological Society of London 2014

Lyell Collection

Downloaded from http://jgs.lyellcollection.org/ at University College Dublin on April 29, 2014
Journal of the Geological Society, London. http://dx.doi.org/10.1144/jgs2013-051
Published *Online First*
© 2014 The Geological Society of London

Brittle structures focused on subtle crustal heterogeneities: implications for flow in fractured rocks

A. M. SODEN[1,2*], Z. K. SHIPTON[1], R. J. LUNN[1], S. I. PYTHAROULI[1], J. D. KIRKPATRICK[3], A. F. DO NASCIMENTO[4] & F. H. R. BEZERRA[4]

[1]*Department of Civil Engineering, University of Strathclyde, Glasgow, G1 1XJ, UK*
[2]*Present address: School of Geological Sciences, University College Dublin, Dublin 4, Ireland*
[3]*Department of Geosciences, Colorado State University, Fort Collins, CO, 80523, USA*
[4]*Department of Geophysics, Universidade Federal do Rio Grande do Norte, Natal, 59078-970, Brazil*
**Corresponding author (e-mail: aisling@fag.ucd.ie)*

Abstract: Host rock mechanical heterogeneities influence the spatial distribution of deformation structures and hence predictions of fault architecture and fluid flow. A critical factor, commonly overlooked, is how rock mechanical properties can vary over time, and how this will alter deformation processes and resultant structures. We present field data from an area in the Borborema Province, NE Brazil, that demonstrate how temporal changes in deformation conditions, and consequently processes, exert a primary control on the spatial distribution and geometric attributes of evolving deformation structures. Furthermore, each temporal deformation phase imparted different hydraulic architecture. The earliest flowing structures are localized upon subtle ductile heterogeneities. Following fault formation, both fault core and damage zone were flow conduits. In later stages of faulting pseudotachylyte welding created a low-permeability fault core and annealed high-permeability fractures within the fault damage zone. Modern flow occurs along a zone of later open shear fractures, defined by the mechanical strength contrast between the host rock and annealed fault. This second hydraulically conductive zone extends hundreds of metres from the edge of the annealed fault damage zone, creating a flow zone far wider than would be predicted using traditional fault scaling relationships. Our results demonstrate the importance of understanding successive deformation events for predicting the temporal and spatial evolution of hydraulically active fractures.

Geometric attributes of faults and fractures (length, orientation and spatial distribution) are of primary importance in predicting fluid flow through fracture networks. For any particular fracture system these attributes are controlled by rock mechanical properties and *in situ* stress at the time of fracture formation. Rock mechanical properties are dependent on the physical conditions (e.g. pressure, temperature, pore fluid) at the time of deformation. Changes in rock mechanical properties can alter deformation processes, and hence deformation structures, during successive phases of deformation. In turn, subsequent deformation phases can reactivate or overprint structures, modifying their mechanical properties. Therefore, fracture networks are not purely stochastic in nature, and the ability to simulate realistic fracture systems depends on coupling accurate statistical quantification of fracture attributes with an understanding of the evolution of the deformation processes, and the attendant structures formed prior to and during fracture formation. This is particularly pertinent to fracture systems in basement terranes that have experienced multiple deformation events. Accurate characterization of fracture population attributes in crystalline rock at both seismic and subseismic resolution is increasingly important as crystalline rocks are targets for nuclear waste repositories (Degnan *et al.* 2003), enhanced geothermal systems (e.g. Sausse *et al.* 2006) and hydrocarbon exploration (e.g. Koning 2003; Schutter 2003; Slightam 2012). Furthermore, containment periods for CO_2 sequestration and nuclear waste storage are so long (between 10^3 and 10^6 years) that predictions of temporally varying rock hydraulic properties (e.g. owing to glacial advance and retreat) are required as input to the safety cases for potential storage or repository sites.

A critical factor, commonly overlooked, is how host rock mechanical properties can vary over time, and how this will alter deformation processes and influence the type, and geometric attributes of, resultant deformation structures. For example, in sandstones, as mechanical strength increases owing to diagenesis, the failure mechanism can change from cataclasis (forming deformation bands) to fracturing (forming joints) (Davatzes *et al.* 2005; Johansen *et al.* 2005). Similarly, fracture attributes such as spacing and length are the product of the host rock mechanical properties at the time of formation (Cooke *et al.* 2006; Moir *et al.* 2010), which may differ from present-day mechanical properties (Shackleton *et al.* 2005; Laubach *et al.* 2009). The impact of diagenetic or depositional processes on host rock properties is evident in along-fault variations in fault zone architecture (e.g. Eichhubl *et al.* 2009; Soden & Shipton 2013). Thus predictions of fracture and fault zone architecture should consider previous mechanical states and not merely the present mechanical state, particularly in areas that have a complex tectonic history.

Furthermore, it is widely recognized that host rock mechanical heterogeneity can influence the spatial distribution of initial deformation structures (Crider & Peacock 2004; Fischer & Polansky 2006), and hence any resulting fault architecture (Childs *et al.* 2009). Contrasts in mechanical strength localize stress (Pollard & Aydin 1988; Moir *et al.* 2013) and act as sites for fracture initiation (McConaughy & Engelder 2001; d'Alessio & Martel 2005) or termination (Cooke *et al.* 2006). What has not been fully explored is the impact of the mechanical heterogeneity created by deformation structures formed under deformation conditions that vary over geological time on subsequent fracture development.

In this study we present data from the Jucurutu fault, located in Jucurutu county in the state of Rio Grande do Norte, NE Brazil. The fault cuts crystalline basement rocks and was initially documented

Downloaded from http://jgs.lyellcollection.org/ at University College Dublin on April 29, 2014

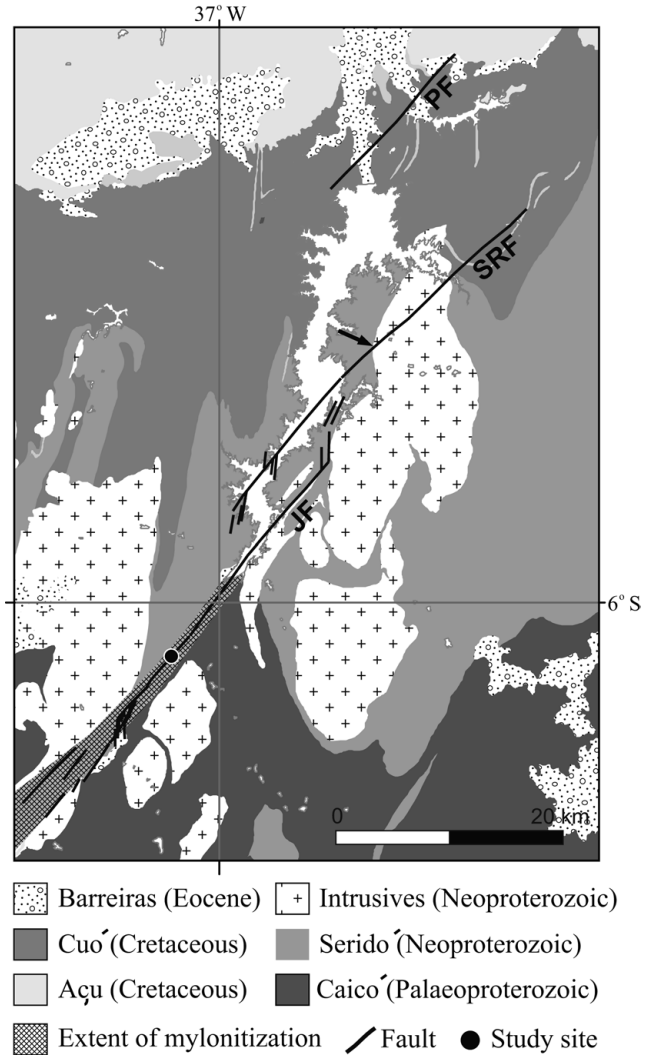

Fig. 1. Map of the Rio Piranhas fault system from satellite images and aerial photographs. The extent of mylonitization associated with the Piranhas shear zone is indicated by cross-hatching. The black arrow indicates the location of observed 150 m apparent dextral offset of a pluton boundary. (Adapted from Kirkpatrick *et al.* 2013.) PF, Rio Piranhas fault; SRF, São Rafael fault; JF, Jucurutu fault.

by Kirkpatrick *et al.* (2013) as part of an investigation of regional fault systems. We have carried out a detailed examination of the structures exposed within a 0.09 km^2 area adjacent to and including the Jucurutu fault, recording structures from the centimetre to hundreds of metres scale. Our data indicate how changes in deformation conditions, and consequently processes, control the observed pattern of deformation structures. We show that in each deformation phase, both the spatial distribution and geometric attributes of the evolving structures are governed by the locations of the structures formed in previous phases. We propose that existing structures act as mechanical heterogeneities, resulting in high stress concentrations that lead to fracture nucleation. This results in discrete temporal episodes of differing, yet related, patterns of hydraulically conductive structures.

Geological setting

Our study examines ductile and brittle deformation structures in Neoproterozoic gneisses of the Borborema Province, NE Brazil (Fig. 1). Regionally the Archaean to Proterozoic basement is cut by a system of steeply dipping, east–west- and NE–SW-trending, dextral strike-slip shear zones intruded by Neoproterozic granites (Vauchez *et al.* 1995; Arthaud *et al.* 2008). The shear zones developed during the Brasiliano orogeny (*c*. 750–540 Ma), and are defined by steeply dipping mylonitic belts hundreds of kilometres long and tens of kilometres wide (Brito Neves *et al.* 2000).

Continental break-up during the Cretaceous generated the Potiguar Basin in the north of the Borborema Province as part of a system of failed rifts. The study area lies on the border of such a rift, the Cariri–Potiguar trend, which extends SW from the edge of the Potiguar Basin (Fig. 1; Matos 1992). Faults bounding the Potiguar basin have throws up to 5 km and are observed on seismic sections to offset the crystalline basement (De Castro *et al.* 2012). On a regional scale the rift faults coincide with the basement mylonitic fabric (Matos 1992; De Castro *et al.* 2008; Kirkpatrick *et al.* 2013). Substantial uplift and erosion of the region during the Cenozoic has exposed the basin margins and deeper parts of the rift systems. Exhumation is interpreted to have occurred at *c*. 90–100 Ma and again post-20 Ma. The former event corresponds to rifting and cooling to temperatures less than 100 °C and the latter to cooling from around 60 °C. Together these are thought to represent *c*. 3 km of denudation (Nóbrega *et al.* 2005; Morais Neto *et al.* 2009).

Our study site is located south of the Potiguar basin within the Piranhas shear zone, a 100 km-scale shear zone that locally trends NE–SW swinging to an ENE–WSW trend further south. We focus on a section of a brittle fault, the Jucurutu fault, which cuts a strongly mylonitized section of the Piranhas shear zone (Fig. 1).

The Jucurutu fault is one of three NE–SW-trending brittle faults that make up the Rio Piranhas fault system. The fault system extends *c*. 150 km along strike, from the Açu reservoir in the north to the Rio do Peixe basin in the south. The only observed offset indicator is a displaced granite pluton boundary on the São Rafael fault, with an apparent dextral offset of the order of *c*. 150 m. No piercing point data exist for these faults, so the dip-slip component of the total slip is unknown. However, observations of slickenlines and corrugations on subsidiary faults indicate net oblique dip-slip offsets (Kirkpatrick *et al.* 2013). Based on interpretation of Landsat images, the Jucurutu fault has a trace length of 40 km and a regional trend 053°. At the regional scale the Jucurutu fault runs parallel to the shear zone, although locally the fault cuts the mylonite foliation at a low angle. Kirkpatrick *et al.* (2013) showed that on the basin scale the geometry of the Jucurutu fault, and other faults of a similar age, is strongly controlled by the pre-existing Brasiliano ductile fabric. However, at the outcrop scale, the mylonitic foliations have only a weak influence on the architecture of the Jucurutu fault zone.

Reservoir-induced microseismic events associated with the São Rafael fault, the northernmost fault in the Rio Piranhas system, also suggest that the spatial distribution of brittle structures is not solely dictated by the pre-existing ductile fabric. Earthquake hypocentres delineate a cloud of microseismicity 2 km long, 230–400 m wide and at depths of 1.5–2 km that coincides with the São Rafael fault, which itself is subparallel to the regional foliation. Pytharouli *et al.* (2011) demonstrated that the microseismicity occurs on multiple fractures some of which are clearly oriented at high angles to the fault and mylonite foliation; the remainder are subparallel to both fault and host rock fabric. In this study we observe laterally extensive, open fractures at high angles to the Jucurutu fault, which we propose are analogous to those hosting the modern-day seismicity recorded at São Rafael.

Field data

The study area at Jucurutu is excellently exposed in the bed of the Piranhas River (Fig. 2). The river inundates the area during the

Downloaded from http://jgs.lyellcollection.org/ at University College Dublin on April 29, 2014

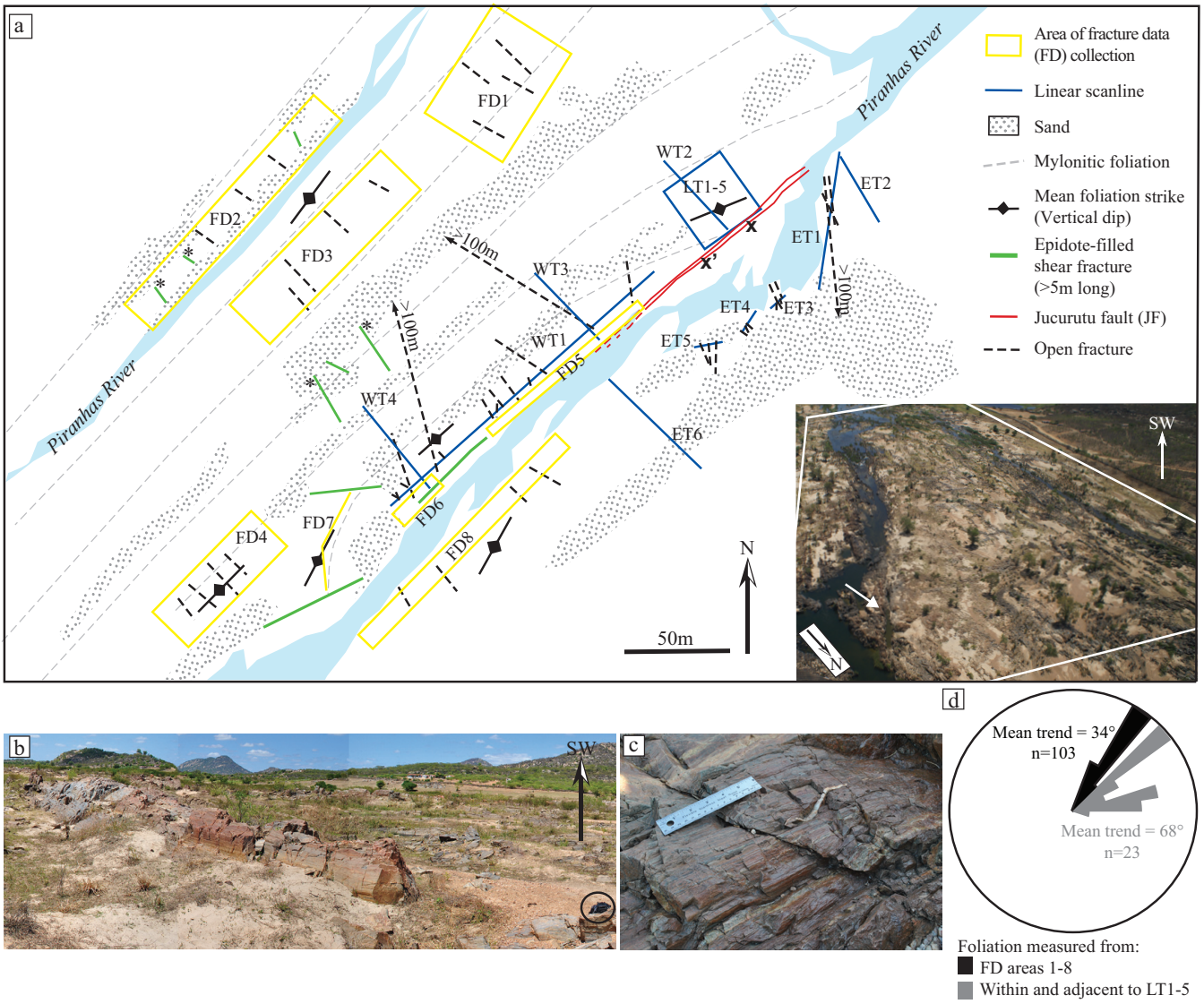

Fig. 2. (**a**) Map of study site showing Jucurutu fault (JF). LT, line transects; box encloses LT1–LT5 oriented parallel to the Jucurutu fault; FD, areas of fracture data collection from ridge outcrops that parallel host rock foliation; fracture data were collected along ridge strike. Asterisks indicate epidote-filled shear fractures offsetting dykes. Inset: Aerial photograph, with study area outlined by white box; white arrow indicates Jucurutu fault core outcrop. (**b**) Typical ridge-like outcrop (FD4) looking SW. Rucksack ringed at bottom right indicates scale. (**c**) Subvertical mylonite foliation. (**d**) Rose diagram of foliation strike.

rainy season but for the remainder of the year is confined to two channels *c*. 10 m wide either side of an 'island' with *c*. 80% outcrop exposure (Fig. 2b).The exposure comprises ridges of intact, smooth crystalline rock, which have been highly polished by the river flow, making sample collection difficult. Mapping at metre scale was carried out using line transects, circular scanlines and base-line mapping, and at 100 m scale from low-altitude aerial photographs (Fig. 2). At the field site, the southerly strand of the Piranhas River runs along the trace of the Jucurutu fault. In one location (around X–X' on Fig. 2), the channel takes a jog to the east, exposing the fault core; elsewhere the central fault core is covered by the channel even in the lowest flow conditions.

At the study site the host rock is a low-grade quartz–feldspar–epidote gneiss that is strongly mylonitized, with a prominent subvertical foliation trending *c*. 034° (Fig. 2c and d). The foliation is defined by compositional banding and by aligned chlorites and muscovites (Kirkpatrick *et al.* 2013). Kinks in the foliation trend define centimetre wide to tens of centimetre wide ductile shear zones oriented subperpendicular to mylonite foliation. These small shear zones represent strain localization after the formation of the main foliation. Additionally, a section of the foliation close to the river is rotated towards a trend of 050° (Fig. 2a and d), suggesting folding of the foliation on the tens of metres scale within the mylonitized zone.

Brittle structures are observed in the study area across a range of length scales from tens of centimetres long fractures to the 40 km long Jucurutu fault. Based on mineral fill and cross-cutting relationships of the brittle structures we suggest that three phases of brittle deformation can be distinguished, which were active under different deformation conditions. The first phase is associated with epidote-bearing fluids, the second occurred at mid-crustal levels under high-stress conditions, and the final phase at shallow levels and in the absence of mineralizing fluids. We present the observations of each fracture generation in the order in which they formed

Downloaded from http://jgs.lyellcollection.org/ at University College Dublin on April 29, 2014

and suggest the deformation condition parameters indicated by the recorded data.

Epidote mineralization is observed in fractures ranging from tens of centimetres long to tens of metres long, in single fractures (Fig. 3a and c) and in en echelon fracture arrays (Fig. 3b). The shortest epidote-filled fractures are found adjacent to the Jucurutu fault core (Fig. 2: LT1–LT5). These fractures are tens of centimetres long, millimetres wide, and form a closely spaced, irregular fracture network (Fig. 3a). Although they have a range of orientations from 000° to 170° (Fig. 4a) the fractures dominantly strike at high angles to the foliation and the Jucurutu fault. The short epidote-filled fractures are largely restricted to the area adjacent to the Jucurutu fault core outcrop and are not as prevalent moving along fault strike to the SE. Rather, epidote-filled shear fractures tens of metres long and 2–10 cm wide are observed along fault strike to the SW and up to 150 m perpendicular to the Jucurutu fault (Figs 2a and 3b, c). Epidote-filled shear fractures adjacent to the Jucurutu fault cross-cut foliation at a low angle (5° and 30°) and are subparallel to the fault trend, whereas those further from the Jucurutu fault are subperpendicular to both the foliation and the fault. The maximum length a single epidote-filled shear fracture was traced for was 42 m, the minimum length was 5 m, but the terminations of the shear fractures were not observed owing to the limited extent of exposures.

The majority of the tens of metres long epidote shear fractures observed display a sinistral shear sense and are associated with localized rotation of the mylonite foliation over centimetres to metre wide zones surrounding the shear fracture (Fig. 3b, d and e). Four of the epidote-filled fractures (Fig. 2a) are associated with sinistrally offset granite dykes, with apparent horizontal separation of between 3 and 9 m. In one instance a section of dyke and gneiss foliation adjacent to the epidote-filled fracture is rotated with a sinistral shear sense; seemingly sheared along the epidote-filled fracture (Fig. 3e). A meshwork of fine epidote veins extends from the epidote-filled fracture into both the gneissic host rock and sheared dyke in a geometry consistent with sinistral slip (Fig. 3f). The dyke may have been sheared either by the ductile shear on which the later brittle fault developed or by the epidote-filled shear fracture under semi-brittle conditions. Two generations of highly indurated gouge can be identified in the epidote shear fractures adjacent to the Jucurutu fault (Fig. 3d). The first generation is composed of millimetre-sized angular to rounded mylonite clasts in an epidote–quartz matrix, whereas the second generation is composed of a fine-grained red gouge tightly cementing clasts of epidote from the first generation gouge.

Epidote fractures and en echelon arrays 1–2 m long are found at a distance of 150 m from the river (FD2 and FD3, Fig. 2a; see also Fig. 3b and c). Centimetre wide ductile shear zones are cut by single epidote-filled fractures that are oriented parallel to the zone of sheared foliation, and by en echelon epidote vein arrays. The overall en echelon array trend parallels the ductile shear zone with single veins cross-cutting the shear zone at a high angle (Fig. 3a–c). Furthermore, in each observed case the en echelon array and ductile shear have the same shear sense.

Epidote mineralization is interpreted as indicating temperatures of *c*. 200–300 °C (Guilbert & Park 1986; Bruhn *et al.* 1994). Assuming a geothermal gradient of 20–30 °C km^{-1} (see Lisker 2004) the abundance and spatial extent of epidote mineralized shear fractures, as well as evidence of cataclasite reworking (Fig. 3d), indicates a significant phase of deformation and associated fluid flow at depths between 7 and 15 km.

The second generation of brittle structures is the Jucurutu fault itself (Fig. 5) and a set of annealed, unmineralized, fractures that occur in the adjacent rock (Fig. 6a and b). Here we define annealed as meaning that fractures do not split when hit with a hammer, and thus are not planes of weakness. We infer that these fractures are closed tight or sealed and are therefore incapable of transmitting fluid at the present day. Fracture aperture is <0.1 mm (indistinguishable with the naked eye), making it impossible to identify in the field if the fractures are mineralized. It was not possible to sample the annealed fractures for thin-section analysis owing to the highly river polished exposure, which made any form of hand sampling away from open joints (where a chisel could be inserted) extremely difficult. Because of the remote location we did not have access to a rock drill. The annealed unmineralized fractures are consistently associated with pseudotachylyte veins that extend from the Jucurutu fault and cross-cut the annealed fractures, indicating that the annealed fractures formed at similar high temperatures and pressures. Although we cannot confirm the actual fracture sealing mechanism we suggest potential mechanisms in our discussion. This does not detract from our main hypothesis, however, as it is not the absolute values of the mechanical properties that affect the localization of future structures but the presence of mechanical heterogeneities with discrete boundaries that act to focus fracture nucleation (Moir *et al.* 2013).

At the study location we define the Jucurutu fault core as the 1.4–2.6 m wide zone of highly indurated, chaotic breccias, bounded by two subvertical planar fault walls dipping *c*. 80° (Fig. 5a and b). The breccias are composed of randomly oriented angular clasts, millimetres to 50 cm in diameter, strongly cemented in a fine-grained purple–grey matrix. No offset markers could be identified along the Jucurutu fault but breccia strands up to 15 m long branching from the fault, oriented *c*. 25–30° counterclockwise to the fault wall, are consistent with sinistral slip (Kirkpatrick *et al.* 2013). Clasts containing fine epidote veins are found in the breccia (Fig. 5c) but no epidote veins are observed to cut the breccia matrix. The matrix itself is composed of epidote and chlorite grains strongly cemented with an aphanitic purple–grey crystalline material. The same aphanitic material fills fractures cross-cutting the breccia clasts and matrix, as well as fractures extending from the core into the host rock immediately adjacent to the core. These fractures have chaotic, cross-cutting orientations and geometries. Differential erosion of the fault breccia has created an irregular surface from which it is possible to sample the clasts, matrix and cross-cutting fractures. Microscopic observations of the aphanitic material from the fault core show it to have characteristics consistent with pseudotachylyte (Kirkpatrick *et al.* 2013). The presence of pseudotachylyte indicates slip at mid-crustal depth as high normal stress promotes frictional melting (Sibson & Toy 2006). The volume of pseudotachylyte and the multiple cross-cutting strands suggest several melt-generating events. The persistence of pseudotachylyte throughout the Jucurutu fault has created a highly indurated fault core; induration and healing of cataclasites by pseudotachylyte is a phenomenon recognized in both field and laboratory settings (Di Toro & Pennacchioni 2005; Griffith *et al.* 2012).

The host rock surrounding the Jucurutu fault is intensely fractured by a high-density, irregular network of closely spaced (<10 cm), tens of centimetres long, unmineralized, annealed fractures (Fig. 6a and b). These fractures cross-cut each other and the tens of centimetres long epidote-filled fractures adjacent to the Jucurutu fault core. The annealed fractures are in turn cross-cut by pseudotachylyte strands extending from the fault core. Annealed fractures have a range of orientations between 000° and 180°, though overall fracture strike is at high angles to the foliation and to the Jucurutu fault (Fig. 6c). Both dextral and sinistral shear sense indicators were recorded (Fig. 6d) and in places conjugate fractures have developed. Annealed fractures were observed along the length of the Jucurutu fault (sampled in FD5, 6 and 7) including surround-

Downloaded from http://jgs.lyellcollection.org/ at University College Dublin on April 29, 2014

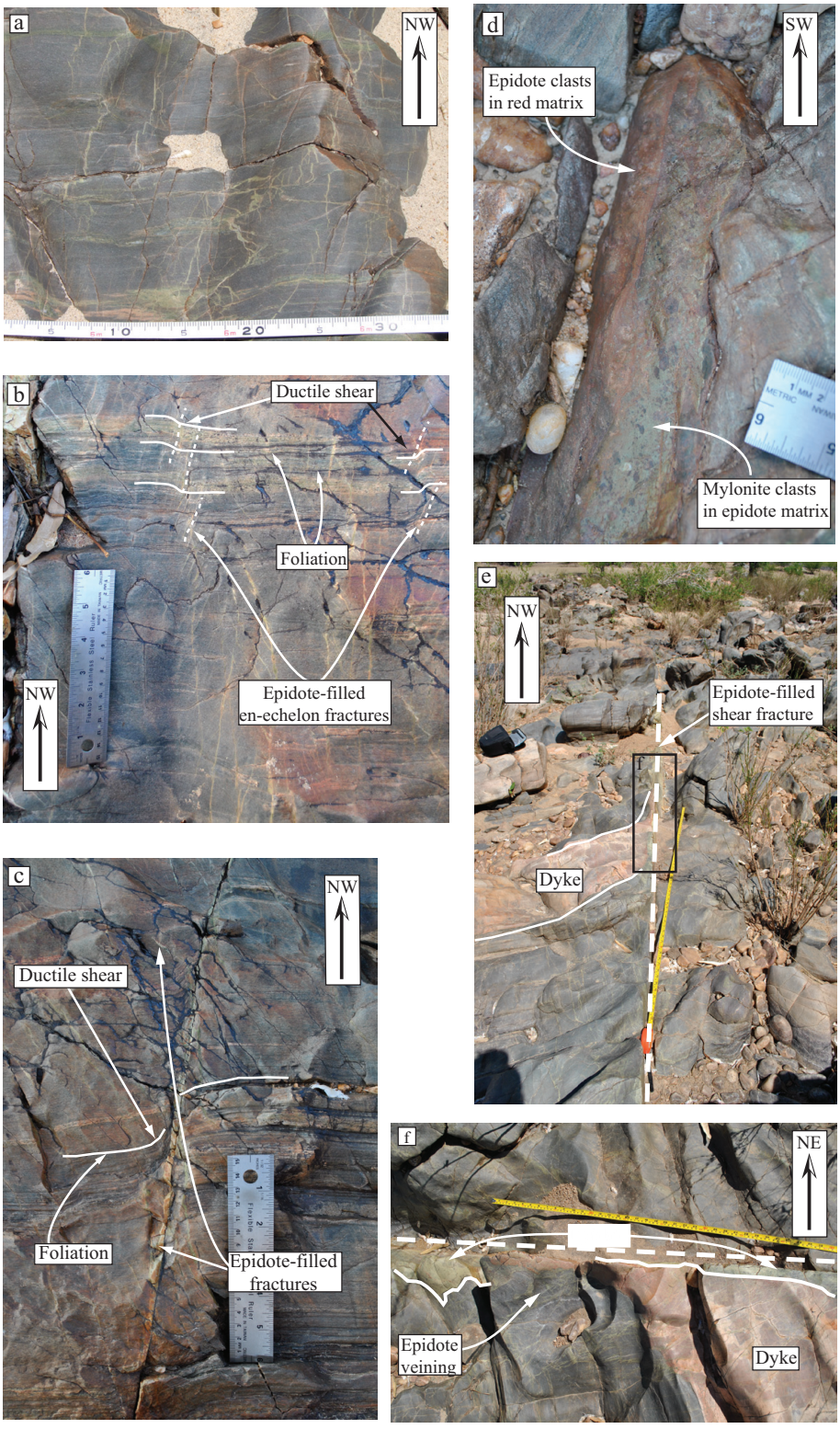

Fig. 3. (**a**) Epidote-filled fractures tens of centimetres long in the Jucurutu fault damage zone. Metre long fractures outside the Jucurutu fault damage zone occur as (**b**) en echelon fractures and (**c**) single fractures seeded on ductile shear. (**d**) Epidote shear fractures >5 m long showing two generations of gouge; the first generation consists of mylonite clasts in a quartz–epidote–chlorite matrix (Kirkpatrick *et al.* 2013), whereas the second generation is composed of epidote clasts in a fine-grained red matrix. (**e**) Sinistral sheared dyke with later (**f**) sinistral epidote-filled fracture.

ing the epidote-filled shear fractures along strike to the SE of Jucurutu fault core exposure (Fig. 2a). No evidence of previous mineralization was observed in any of the annealed fractures.

The intensity of fracturing in the host rock along Jucurutu fault strike was measured using circular scanlines along five line transects perpendicular to the fault core (Fig. 2a). On each line transect circles 1 m in diameter were spaced at 4–8 m intervals, depending on exposure. Background joint density was measured using circular scanlines at locations 210 and 160 m from the Jucurutu fault, on the west and east bank respectively. All visible fractures intersecting the circle were counted, with no differentiation made between epidote-mineralized and unmineralized, annealed fractures. As fractures

Downloaded from http://jgs.lyellcollection.org/ at University College Dublin on April 29, 2014

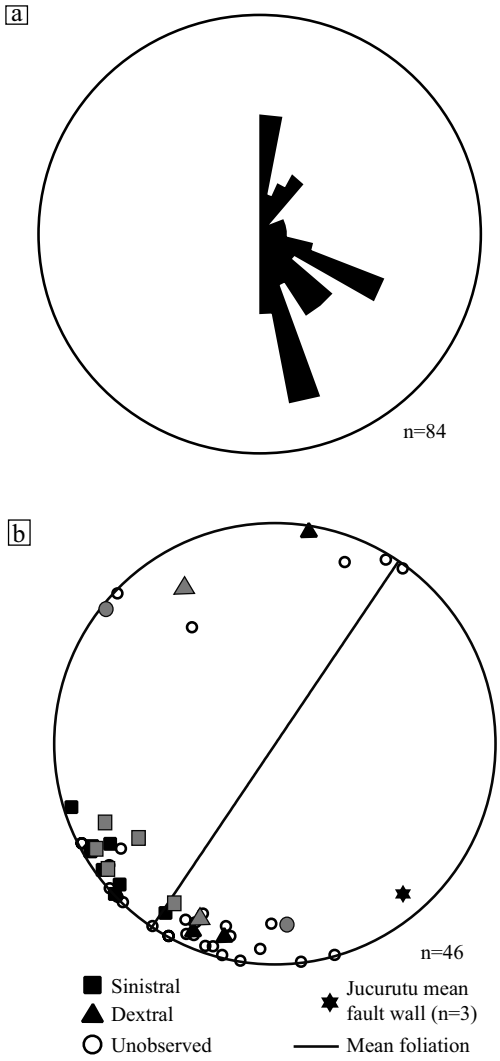

Fig. 4. (**a**) Rose diagram of tens of centimetres long epidote-filled fractures in the Jucurutu fault damage zone, recorded from LT1–5. (**b**) Stereonet of epidote-filled fractures and shear sense where observed. Grey symbols are epidote-filled shear fractures >5 m long, shown in Figure 2a. Mean mylonite foliation $n = 103$, with standard deviation of 13. It should be noted that the epidote-filled fractures strike at a high angle to the mylonite foliation.

intersecting the circle were counted rather than fractures terminating within the circle, the measure obtained is for fracture intensity rather than fracture density (Mauldon *et al.* 2001). On the west bank background fracture intensity is 10 fractures m^{-1} and on the east bank 16.5 fractures m^{-1}. Fracture intensity decreases outwards from the fault core, from a maximum of 58 fractures m^{-1}, reaching background levels between 40 and 60 m from the fault wall (Fig. 7). The spatial distribution of fractures in a zone of high-intensity, chaotic fracturing surrounding the Jucurutu fault defines the fault damage zone, which we interpret to have formed during slip on the Jucurutu fault. Damage zone width and fracture intensity is heterogeneous along fault strike. On average, fracture intensity along WT4 is twice background levels, whereas WT2 records fracturing almost three times background value.

The third and final generation of deformation structures is composed of open shear fractures (Fig. 8a) and open fracture zones metres to tens of metres long (observed in well-exposed areas FD1–FD4 and FD8; Fig. 2). Open fractures have apertures ≥1 mm and no mineral fill or staining (Fig. 8b and c). Occurring outside the Jucurutu fault damage zone, their geometric properties are in contrast to the dense, cross-cutting, annealed fracture network and short epidote-mineralized fractures observed in the Jucurutu fault damage zone. Open fractures and fracture zones are more widely spaced (Fig. 8a), oriented subparallel to each other and at a constant high angle to foliation (Fig. 9). All observed open fractures have near-vertical dips. At least three isolated open fracture zones were observed in the Jucurutu fault damage zone, but in general where the annealed meshwork fractures are present adjacent to the Jucurutu fault the open fractures are absent (Fig. 7a). No open fractures or fracture zones were observed cutting the Jucurutu fault core. Three of the open fracture zones were traced over 100 m from the edge of the annealed Jucurutu fault damage zone (Fig. 2 WT and ET transects), and a further 18 open fractures were traceable for between 10 and 20 m. However, owing to sand cover the terminations of neither single open fractures nor fracture zones were observed.

Open shear fractures and en echelon fracture arrays crosscut centimetre-scale epidote veins (Fig. 10a) and ductile shear zones (Fig. 10a), and nucleated at the edges of epidote-filled shear fractures (Figs 8d and 10b). The open en echelon arrays share the same trend as the ductile shear zones and epidote veins, and those open fractures nucleating at the edges of epidote-filled shear fractures form at a high angle to the shear fracture. Both apparent dextral and sinistral shear sense indicators are observed (Fig. 9b) consistent with normal reactivation, whereby only a minor reorientation of the stress field will result in a change in the apparent slip direction in the horizontal exposure.

Structural and hydraulic evolution

Based on the field data we have developed a conceptual model for the structural and hydraulic evolution of the fault and fracture system at Jucurutu (Fig. 11). The crystalline basement has experienced multiple deformation phases under deformation conditions that evolved through time. The deformation structures observed at the study site are consistent with deformation occurring under progressively decreasing temperatures (Fig. 12). Initial deformation was ductile and occurred at greenschist-facies conditions during the Brasiliano orogeny. Subsequently brittle deformation was associated with epidote mineralization and pseudotachylyte formation as the area experienced rift-related extension and exhumation during the Cretaceous (Kirkpatrick *et al.* 2013). Although the exact timing of open fracture formation is unclear in the absence of mineralizing fluids, the crosscutting relationships and trends of the open fractures show that they formed later than the Jucurutu fault damage zone, presumably at lower stresses during Cenozoic exhumation. As deformation conditions changed so too did the deformation processes and consequently the type of structure formed. Each generation of structure created a discrete mechanical heterogeneity within the host rock that acts as a nucleation site for later structures, rather than structures exploiting the mechanical anisotropy of the mylonitic fabric (Shea & Kronenberg 1993; Tien *et al.* 2006). This observation of fracture nucleation on discrete mechanical boundaries is in keeping with the numerical modelling results of Moir *et al.* (2013). Our observations support a conceptual model with four distinct phases of deformation, each later phase being affected by the presence of prior deformation structures.

The initial phase of deformation during the Brasiliano orogeny formed the regional Piranhas shear zone. Observations of synkinematic growth of chlorite and muscovite, and crystal-plastic deformation of quartz and plagioclase, indicate mid-crustal, greenschist-facies

Downloaded from http://jgs.lyellcollection.org/ at University College Dublin on April 29, 2014

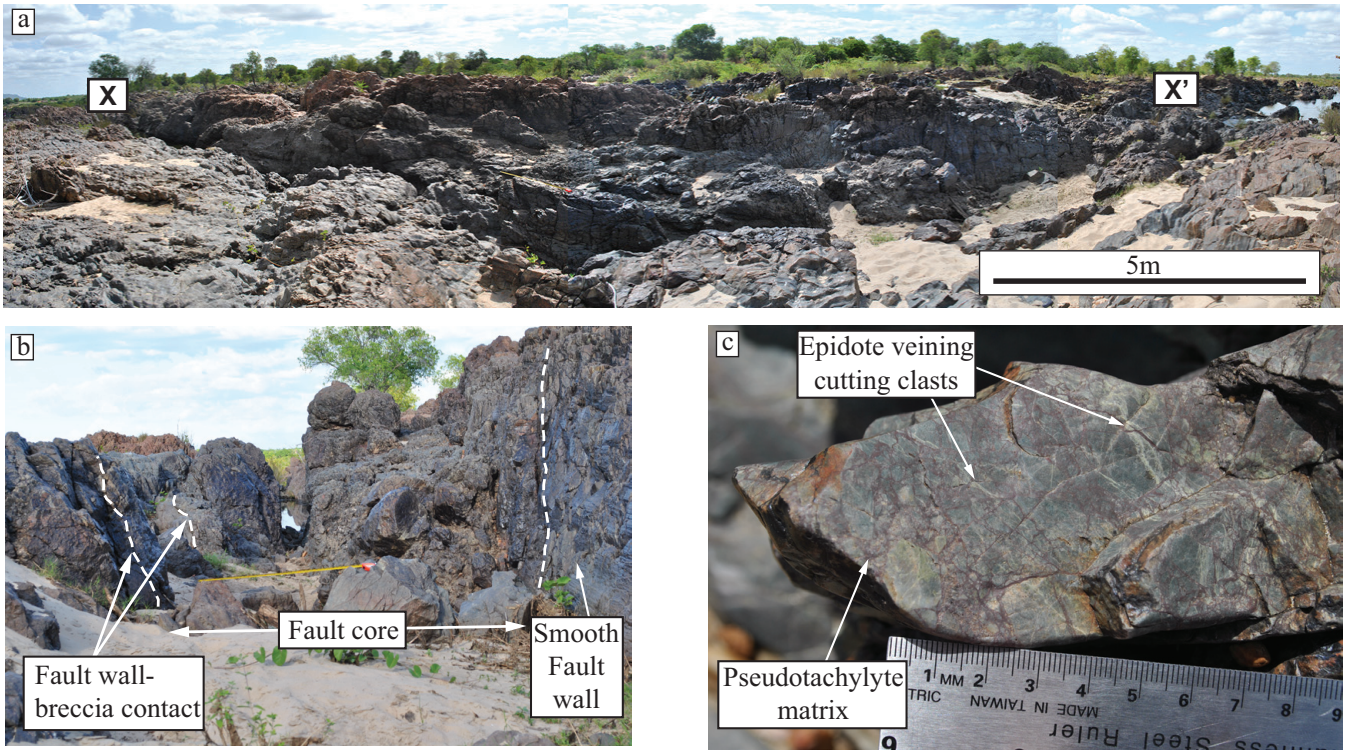

Fig. 5. (**a**) A *c*. 20 m long strike-parallel section of the Jucurutu fault core exposed in the Piranhas river gulley (location marked X–X' in Fig. 2a). (**b**) Fault core width ranges from 1.4 to 2 m. No principal slip surface is exposed (it is presumed to be weathered out in the gully) but breccias are bounded by smooth fault walls. Clasts are randomly oriented and up to 0.5 m wide. Tape measure is 1 m long. (**c**) Close-up of Jucurutu fault breccia, which is strongly welded by pseudotachylyte. It should be noted that epidote fractures within clasts do not cross-cut the purple matrix of the breccia.

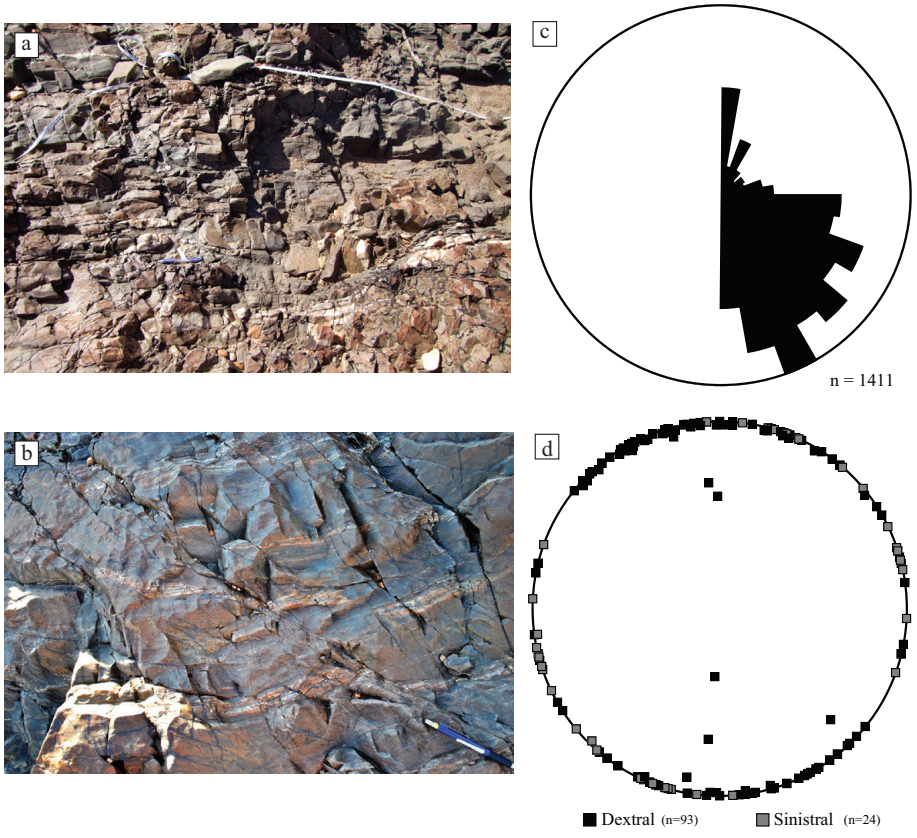

Fig. 6. Jucurutu fault damage zone. (**a**, **b**) High-density tens of centimetres-scale unmineralized annealed fractures. (**c**) Rose diagram of unmineralized annealed fracture strike from LT1-5, FD5, 6 and 7 and (**d**) poles to annealed fractures for which shear sense indicators were observed. It should be noted that in the Jucurutu fault damage zone annealed unmineralized fractures are more common than epidote-filled fractures.

Downloaded from http://jgs.lyellcollection.org/ at University College Dublin on April 29, 2014

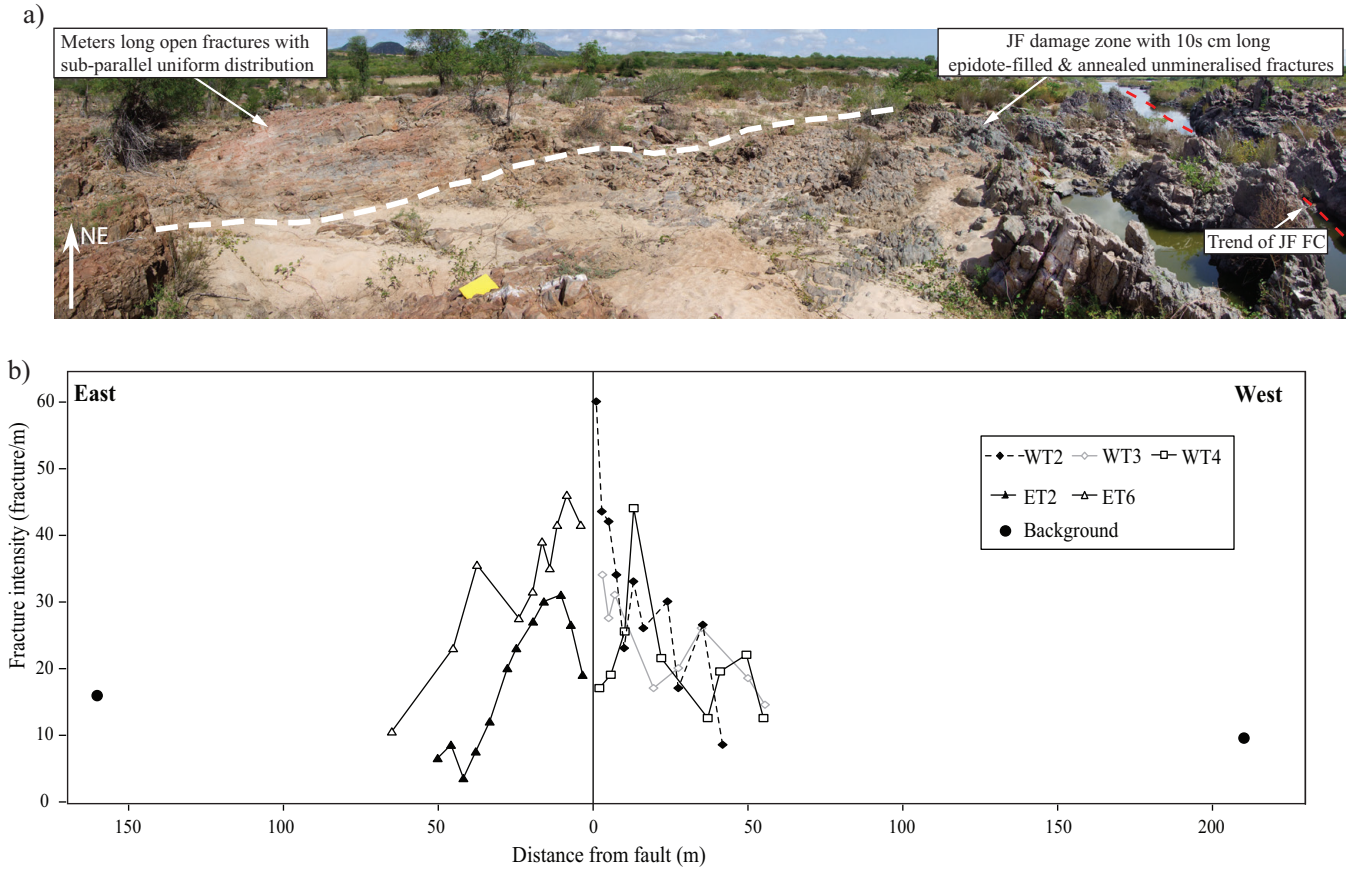

Fig. 7. (**a**) View of transition from short, meshwork fracturing developed in the damage zone of the Jucurutu fault to dominantly subparallel long open fracture and fracture zones that characterize the area extending from the edge of the damage zone outwards across the rest of the study area. JF FC, Jucurutu fault core. (**b**) Joint intensity data collected using circular scanlines at 4–8 m intervals along line transects perpendicular to the Jucurutu fault.

conditions and temperatures of up to *c*. 450 °C (Kirkpatrick *et al.* 2013). Within the mylonitized zone, further localization of strain formed broad tens of metres-scale folds, as suggested by the foliation rotation from 30° to 50° adjacent to the Jucurutu fault, down to centimetre wide ductile shear zones (Fig. 11a).

Epidote-bearing structures at the centimetre and metre scale are localized on ductile shear zones, indicating that the ductile shear zones acted as mechanical heterogeneities on which the fractures initiated (Fig. 11b). The epidote-filled structures are themselves crosscut by unmineralized, annealed and open fractures, indicating that the epidote-filled shear fractures formed during the earliest phase of brittle deformation. Assuming a geothermal gradient of 20–30 °C km^{-1} the epidote-filled faults are interpreted as having formed at depths of between 7 and 15 km.

At the tens of metres scale the mylonite foliation, adjacent to the Jucurutu fault core, is rotated 20° clockwise. Coincident with rotation away from the main orientation are the tens of centimetres long epidote-filled fractures, and along fault strike to the SW are the longest epidote-filled faults observed in the study site (Fig. 2a). We suggest that this concentration of epidote-bearing structures is associated with the rotation of foliation at the tens of metres scale. Folds acted as heterogeneities on which fractures localized, similar to the centimetre- and metre-scale ductile shear zones. These processes resulted in the formation of an epidote-bearing fault and zone of epidote fault strands and attendant off-fault epidote fractures prior to formation of the Jucurutu fault (Fig. 11b).

The presence of epidote in the Jucurutu fault core matrix and as epidote veins in breccia clasts suggests that the Jucurutu fault localized on a pre-existing epidote-rich fault (Fig. 11c). The absence of epidote-filled fractures or larger epidote remnants in the Jucurutu fault core suggests that the fault accumulated sufficient slip to fully rework the epidote-rich fault material, via attrition and cataclasis. Therefore we propose that the epidote-associated deformation phase ceased either prior to or in the early stages of Jucurutu fault development. The abundance of pseudotachylyte in the Jucurutu fault indicates fault slip at mid-crustal levels under high shear stress conditions (Sibson & Toy 2006). The lack of mineralization suggests dry conditions (at least transiently), consistent with high effective stresses that promote frictional melting. In the Jucurutu fault damage zone the annealed unmineralized fractures cross-cut the epidote-filled fractures and probably formed in the same stage as the pseudotachylyte. Pseudotachylyte generation strongly welded and annealed the Jucurutu fault fault breccia (Fig. 11d). The annealed fracture surfaces indicate that the surrounding rock volume was also indurated post-displacement. As stated above, we are unable to determine the mechanism of fracture annealing; however, experimental studies of closed fractures in seismogenic fault damage zones (e.g. Tenthorey & Cox 2006; Tenthorey & Fitz Gerald 2006) suggest that fractures may have been healed by hydrothermal reactions and mineral precipitation. Furthermore, these studies find a significant increase in cohesive strength of fault zones as a consequence of the healing process (Tenthorey & Cox 2006).

Downloaded from http://jgs.lyellcollection.org/ at University College Dublin on April 29, 2014

Fig. 8. (**a**) Single open fractures transecting FD4. (**b**) Tens of metres long open en echelon fracture zone and (**c**) open en echelon fracture zone and single fractures. All occur *c*. 100 m outside limit of Jucurutu fault damage zone.

A regional apatite fission-track study (Morais Neto *et al.* 2009), including a sample location adjacent to our study site, indicates two past cooling events. The first event cooled through 100 °C at *c.* 100 Ma and a second since 20 Ma cooling through 60 °C (Fig. 12). For a geothermal gradient of 20–30 °C km^{-1} (see Lisker 2004) the event at 100 Ma indicates when rock now exposed at surface was at depths of 3–5 km. Observations of the Jucurutu fault rocks suggest that they formed at >200 °C and therefore by 100 Ma; thus the Jucurutu fault was active during the Cretaceous rifting (Kirkpatrick *et al.* 2013).

The final deformation phase formed open, unmineralized fractures, but did not reactivate the Jucurutu fault. None of the open fractures cut the fault breccia or fault walls. Instead, open shear fractures initiated either at the edge of the welded Jucurutu fault damage zone or on existing ductile or epidote-filled shear fractures outside the Jucurutu fault zone (Fig. 11e). Therefore we propose that mechanical contrasts created by structural heterogeneities, from centimetre-scale ductile shear zones to the tens of metres-scale indurated Jucurutu fault core, acted as sites of joint initiation. The presence of dextral and sinistral apparent shear sense indicators on fractures with near-vertical fracture dip suggests that the open fractures formed at shallow depths in a stress field consistent with normal fault slip. These open fractures may have resulted from the phase of exhumation suggested by Nóbrega *et al.* (2005) and Morais Neto *et al.* (2009), thought to have occurred at *c*. 20 Ma.

Our model demonstrates how temporally evolving deformation conditions can generate complex, hierarchical fault architectures by forming generations of deformation structures that vary in their mechanical and geometric properties. Each structure generation imparts a particular mechanical heterogeneity to the host rock that influences the spatial distribution and geometry of later structures. For example, the formation of pseudotachylyte in the Jucurutu fault indurated the fault core, which subsequently acted as a stiff inclusion in the country rock. Furthermore, each generation of deformation structures imparted different hydraulic architectures (Fig. 11). The earliest flowing structures were the epidote-bearing fractures, which are likely to have been mineralized during the early stages of deformation associated with the Jucurutu fault (Fig. 11b). Abundant epidote in the fault core cataclasites of the Jucurutu

Downloaded from http://jgs.lyellcollection.org/ at University College Dublin on April 29, 2014

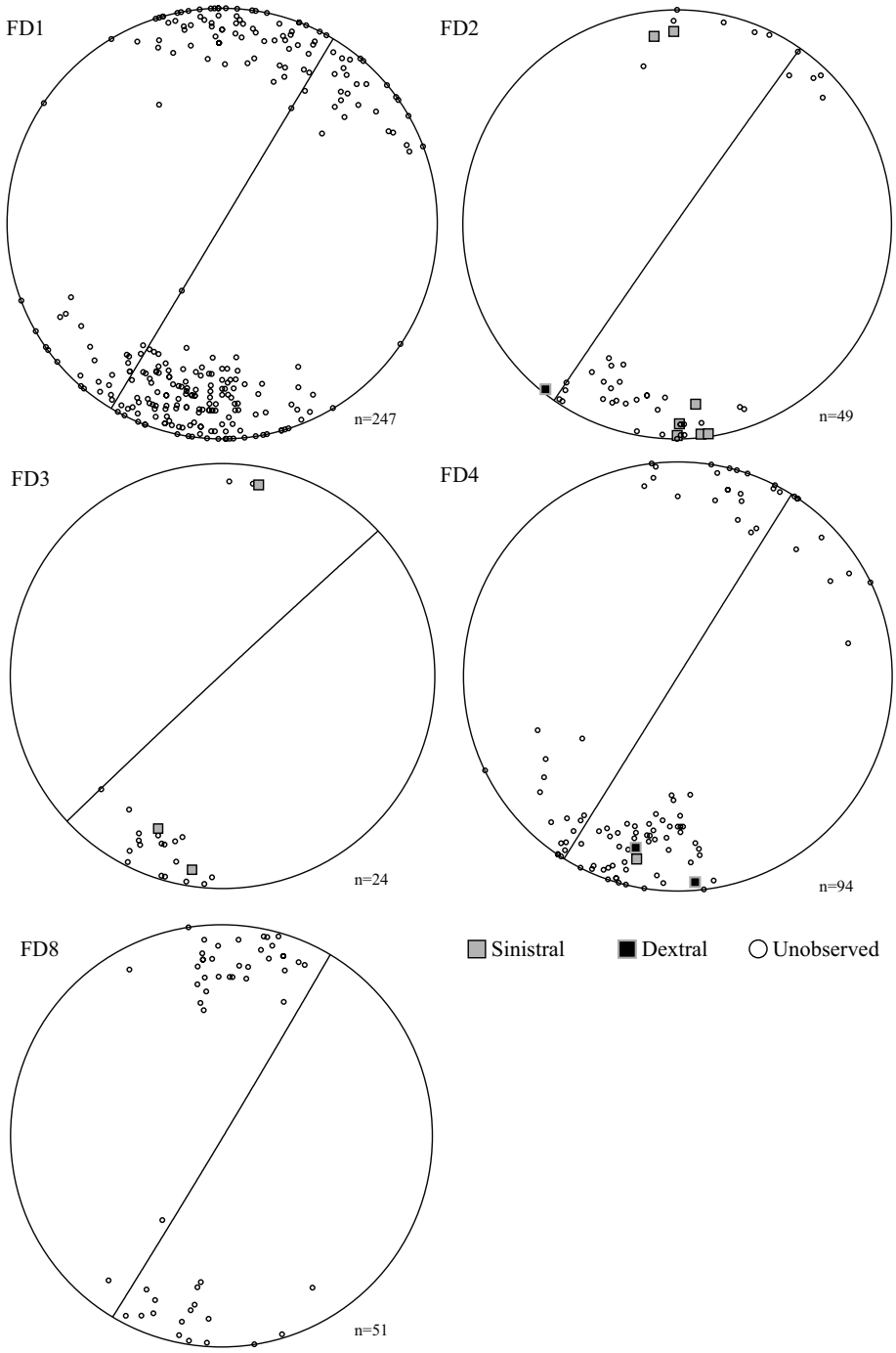

Fig. 9. Stereonets of open fractures and fracture zones from sample areas FD1–4 and FD8. Great circle is mean mylonite foliation from each sample area. Open fractures with shear sense indicators are highlighted.

fault attests to fluid flow also occurring in the fault core during deformation (Fig. 11b) Pseudotachylyte welding of the Jucurutu fault in the later stages of development resulted in a very low-permeability fault core, with flow focused in the surrounding fractured damage zone that was created during fault growth (Fig. 11c). Modern flow occurs at depth along the long open shear fractures and fracture zones that extend from the edge of the annealed Jucurutu fault damage zone (Fig. 11e). These act like a secondary hydraulically conductive fault zone, adjacent to the original fault damage zone. This secondary zone surrounds the annealed fault damage zone and is far wider than would be predicted using fault scaling relationships; this and the implications for developing predictive flow models are discussed below.

Discussion

The role of pre-existing structures in influencing fracture and fault formation has been previously recognized (Crider & Peacock 2004). Moreover, it is widely accepted that faults are inherently weak and, as pre-existing weaknesses, will be reactivated in subsequent deformation events (Holdsworth *et al.* 2001; Butler *et al.* 2008). However, what has not been examined in depth is the effect that evolving deformation conditions (stress state, temperature, availability of fluid) have on structure formation during successive deformation phases. As conditions change so too do the deformation processes, and hence the mechanical and geometric properties of the resultant deformation structures. Thus each generation of

Downloaded from http://jgs.lyellcollection.org/ at University College Dublin on April 29, 2014

Fig. 10. (**a**) En echelon fractures nucleating on a epidote vein (inset (**b**). (**c**) En echelon open fractures and (**d**) open fractures nucleating on epidote mineralized fractures, which themselves overprint ductile shear zones.

structure exerts a distinct influence upon the formation of successive structures, acting as mechanical heterogeneities that control the geometric attributes of new structures in a particular manner. Ultimately, as deformation occurs in an evolving tectonic setting, the degree of mechanical and structural heterogeneity, and thereby the complexity of the fault zone architecture, increases, but not in a manner that would be predicted from conventional fault scaling relationships or fault zone models.

Fault scaling relationships indicate broad positive correlations between increasing fault displacement and deformation in the form of increasing fault core and damage zone width (Shipton *et al.* 2006; Childs *et al.* 2009) and increasing fracture density in the damage zone (Chester & Chester 2000; Wilson *et al.* 2003), as well as decreasing damage zone fracture density with increasing distance from the fault (Schultz & Evans 1998; Sleight *et al.* 2001; Chester *et al.* 2004; Savage & Brodsky 2011) with a coincident decrease in bulk permeability (Mitchell & Faulkner 2012). However, fault-scaling relationships provide only a generalized description of fault zone attributes (Manzocchi *et al.* 2010); for example, in the case of fault width there are three orders of magnitude scatter for any value of displacement (Shipton *et al.* 2006). Furthermore, global scaling relations simplify fault zone geometry by omitting factors such as spatial or temporal variations in rock mechanical properties. Nevertheless, despite these limitations, these relationships are frequently applied in reservoir flow models (Yielding *et al.* 1997; Hesthammer & Fossen 2000; Jolley *et al.* 2007; Myers *et al.* 2007; Slightam 2012).

Downloaded from http://jgs.lyellcollection.org/ at University College Dublin on April 29, 2014

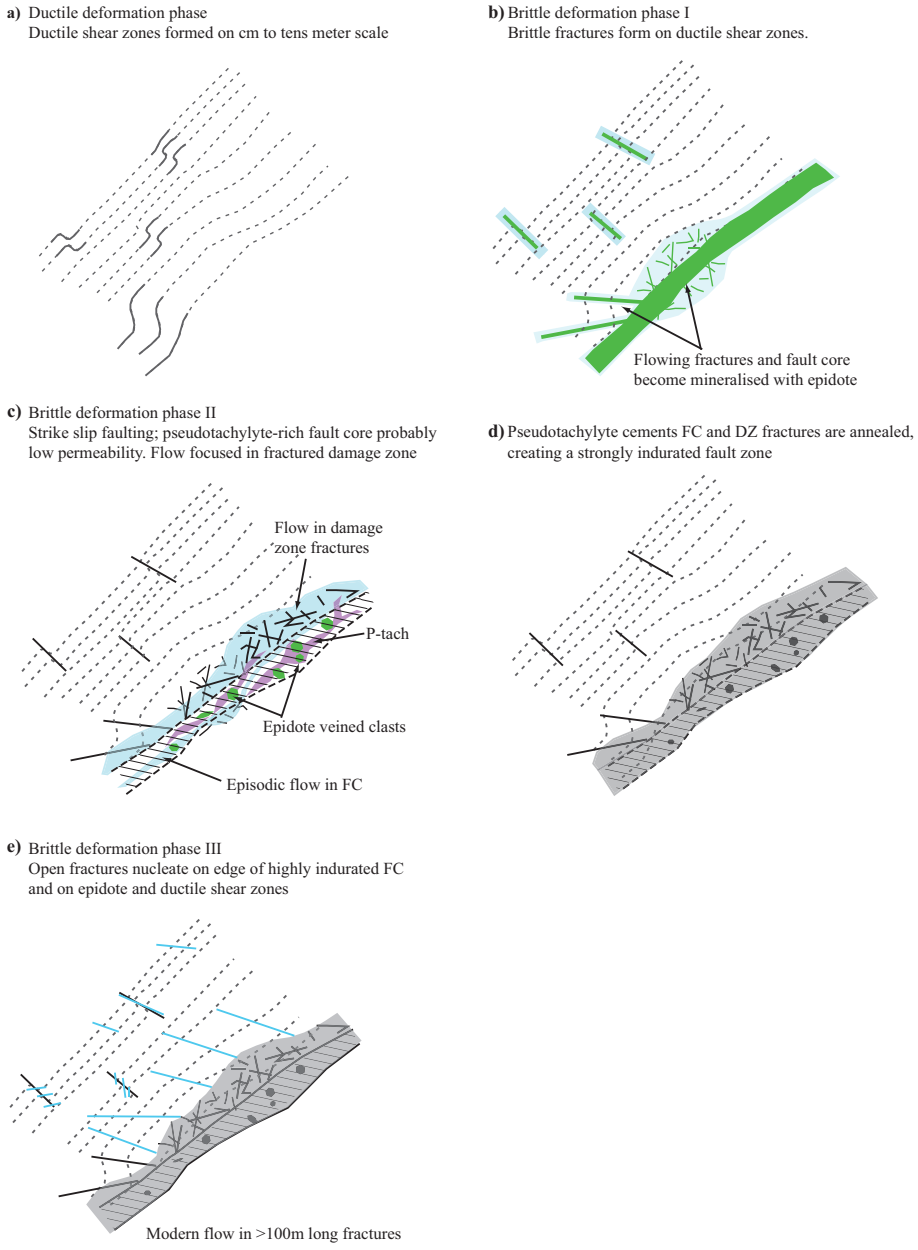

Fig. 11. Conceptual model of fault and fracture system structural evolution and impact on hydraulic architecture. Temporal evolution of deformation conditions leads to variable deformation processes and hence mechanically and spatially distinct generations of deformation structures. FC, fault core; DZ, damage zone.

Models of fault zone and hydraulic architecture in crystalline rocks commonly assume an intensely fractured fault and damage zone that forms a high-permeability corridor relative to the low-permeability host rock (Caine *et al.* 1996; Evans *et al.* 1997; Younes *et al.* 1998; Slightam 2012), although the behaviour of the fault zone as either a conduit or barrier to flow will depend on a variety of factors; for example, the stress state relative to fracture orientation (Henrikson & Braathen 2006; Agosta *et al.* 2010) and mineralization (Eichhubl *et al.* 2009). Fault zones in crystalline rock are generally assumed to be mechanically weak zones and thus easily reactivated, making them preferential flow paths that may exhibit multiple mineralization phases (Le Garzic *et al.* 2011). In a strongly anisotropic rock such as mylonite the tectonic foliation is suggested to exert a significant influence on the location and geometry of brittle faults (Beacom *et al.* 2001; Butler *et al.* 2008), as the foliation creates planes of weakness that can be exploited by fracturing (Shea & Kronenberg 1993).

Fracture network models are constructed from statistical descriptions of fracture set attributes (length, orientation, spacing) obtained from site-specific seismic surveys, outcrops and boreholes (Aliverti *et al.* 2003; Degnan *et al.* 2003; Sanders *et al.* 2003). However, seismic surveys even of the highest resolution are incapable of imaging metre-scale fractures, and outcrop and borehole data are unavoidably sparse and incomplete (Belayneh *et al.* 2009). Thus the fracture network model may not fully capture the complexity of the fracture pattern or may overlook important hydraulic conduits.

Although scaling laws and generic fault models are useful, we have shown the impact that temporal and spatial variation in rock mechanical heterogeneity has on structure evolution and as a result the hydraulic architecture of fault-related fracture systems. Our data demonstrate that structural heterogeneities across a range of length scales and in some cases with a subtle expression, such as the minor ductile shear zones, and not the pre-existing fabric influence the geometric attributes of successive deformation structures.

Downloaded from http://jgs.lyellcollection.org/ at University College Dublin on April 29, 2014

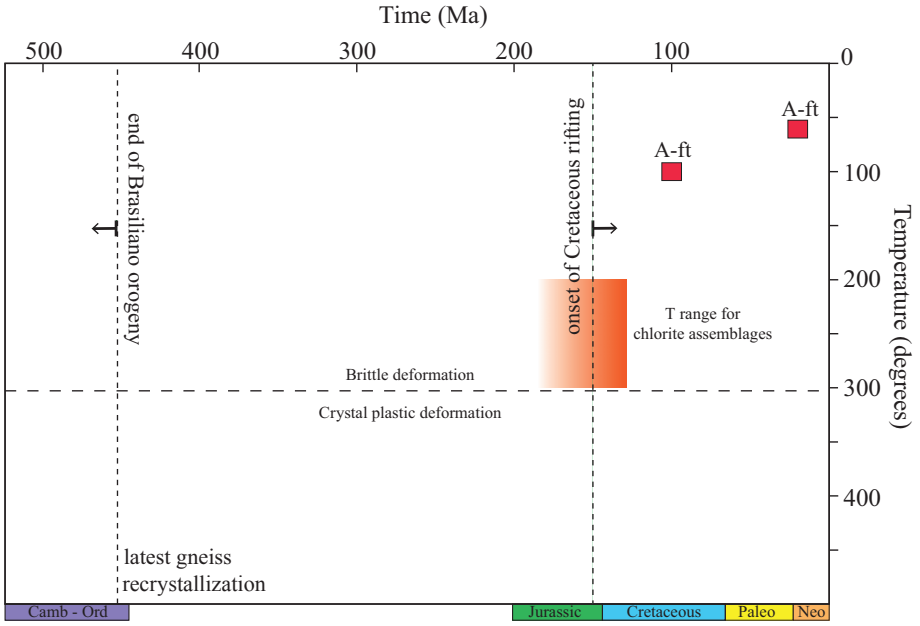

Fig. 12. Temperature–time graph indicating timing of ductile and epidote-associated deformation phase, upper and lower temperatures for epidote-associated deformation (chlorite assemblages) and apatite fission-track temperatures (A-ft) for 100 and 20 Ma cooling events.

Tens of centimetres wide ductile shear zones formed at high angles to the regional mylonite foliation. The epidote-filled shear fractures developed parallel to these ductile shear zones and consequently cut the regional foliation at high angles. We suggest that rotations of the mylonitic foliation at the tens of metres scale indicate a broad fold that acted in the same manner as the centimetre-scale ductile shear zones, as a mechanical heterogeneity on which epidote shear fractures and later the Jucurutu fault localized. Although at the regional scale the Jucurutu fault is parallel to the Piranhas shear zone (Kirkpatrick *et al.* 2013), at the study site the fault cross-cuts the fabric at low angles. Continued evolution of deformation conditions resulted in pseudotachylyte cementation and annealing of the Jucurutu fault, and its surrounding damage zone, creating a strong fault zone that was not reactivated in the last phase of deformation. Instead, the indurated fault zone presented a mechanical contrast to the host rock that promoted nucleation of open shear fractures along its contact with the gneissic host rock.

In the most recent phase of deformation the geometric attributes of the open shear fractures are controlled by all three prior generations of deformation structure. Open fractures initiate on the edges of both epidote-filled shear fractures and ductile shear zones. Epidote-filled fractures act as sites of initiation for en echelon arrays of open joints. Open shear fractures up to hundreds of metres long extend from the edge of the indurated Jucurutu fault. For all prior deformation structures the mechanical contrast between the pre-existing structures and the host rock concentrates stress, promoting open fracture formation. The formation of open joints on ductile shear zones, epidote shear fractures and on the edge of the Jucurutu fault zone rather than the reactivation of the main fault surface or off-fault fractures is inconsistent with the view of weak fault zones being preferentially reactivated in later deformation events.

In this study the evolution of deformation conditions and processes has culminated in the formation of a second hydraulically conductive fault damage zone of open low-offset shear fractures, adjacent to the original Jucurutu fault damage zone, the location and size of which might be overlooked by typical fracture surveys. Line transects perpendicular to the fault indicate fault-related fractures reaching a constant lower limit (the edge of the damage zone) *c*. 60 m from the fault (Fig. 8), whereas the high-angle open fractures extend beyond the 150 m wide exposure from the main fault. These low-offset shear fractures would not be identified by seismic surveys, and boreholes would be unlikely to identify them as a fault-related zone. Therefore, the area of greatest permeability would be assumed to occur within the *c*. 120 m wide damage zone surrounding the Jucurutu fault core.

Furthermore, as the width of this wide zone of open fault-related fractures is not directly related to the displacement accrued by the Jucurutu fault, the true lateral extent of the open shear fracture zone may not be predicted from fault scaling relationships. Assuming the Jucurutu fault has a minimum displacement of 150 m, similar to that observed on the São Rafael fault, the global scaling relationship for damage zone thickness with displacement (Savage & Brodsky 2011; Torabi & Berg 2011) would suggest a maximum damage zone width of *c*. 700 m. However, the line-transect fracture data indicate that the limit of the damage zone is *c*. 60 m either side of the Jucurutu fault, giving a total damage zone width of 120 m, which, according to the scaling relationship, correlates with a fault displacement of 150 m. Therefore the scaling relationship suggests that the damage zone as defined by the fracture scanline data is most probably the limit of the fault-related fracturing and, consequently, the principal hydraulically conductive zone would go unnoticed.

Our proposition that these open fractures are an important along-fault hydraulically conductive zone is supported by the microseismic data associated with the São Rafael fault (Pytharouli *et al.* 2011) to the north of the Jucurutu fault (Fig. 1). Microseismic events at São Rafael are triggered by pressure diffusion from the reservoir, thus occurring on open flowing fractures. The microseismicity defines multiple open flowing shear fractures, several hundred metres in length in a longitudinal zone parallel to and coincident with the main São Rafael fault trace. These shear fractures have orientations both parallel and at high angles to the São Rafael fault and the mylonitic foliation. We propose that the hundreds of metres long open shear fractures observed at the Jucurutu study site are analogous to those at São Rafael and, given their length, are potentially significant hydraulically conductive fractures.

This study shows that the most hydraulically important aspect of the fault system may go undetected or be underestimated. The largest existing fault structures may not be reactivated as commonly

Downloaded from http://jgs.lyellcollection.org/ at University College Dublin on April 29, 2014

expected, and the resulting flow network is not always well described by fault zone scaling relationships. Hence, an important consideration in the development of realistic fracture flow models is the mechanical heterogeneities of the rock across a range of scales and their impact on the fracture formation and geometric attributes.

We have demonstrated that deformation under multiple conditions alters the mechanical properties of structures and leads to an increase in structural complexity. Recent improvements in thermochronology have shown that episodic burial and exhumation histories may be more common than monotonic cooling and unroofing (e.g. Holford *et al.* 2010). Therefore when investigating recent brittle fault formation in a long-lived tectonic setting we should consider previous deformation phases, conditions and resultant structures, as they may have a bearing on the formation and architecture of the more recent faults and fracture networks.

Conclusions

Temporal changes in deformation conditions (pressure, temperature and availability of fluids) and thus deformation processes in the study area created generations of structures that differ in their mechanical and geometric attributes. These structures behaved as mechanical heterogeneities within the host rock, strongly influencing the spatial distribution and geometric attributes of structures formed in later deformation events. Mechanical contrasts at a range of scales and types, from centimetre wide ductile shear zones to the hundreds of metres scale welded Jucurutu fault, influence the formation of subsequent structures, culminating in the generation of extensive open shear fractures and fracture zones. Hence, deformation under evolving conditions produces an increasingly mechanically heterogeneous and complex fracture system architecture.

In addition to differing frequency and spacing of deformation structures, the successive deformation events were characterized by different hydraulic structures. The earliest flowing structures, the epidote-filled fractures, are perpendicular to the mylonitic foliation. Hence, rather than reactivating the regional foliation the epidote-filled fractures formed parallel to foliation in centimetre wide ductile shear zones. The Jucurutu fault cross-cuts the mylonitic fabric at a low angle and both fault core and damage zone were flow conduits. However, pseudotachylyte welding created a highly indurated, low-permeability fault core and damage zone. Conventional methods for predicting shear fracture and fracture geometric attributes would focus on applying fault-scaling relationships to the larger brittle structures. Thus the most recent phase of fracturing would be assumed to have reactivated the Jucurutu fault and increased the fracture density in, and the width of, the Jucurutu fault zone. The open shear fractures and joints, which are controlling flow at depth, lie outside the damage zone of fault-related fractures, which would, by current fault models, define the lateral extent of the Jucurutu fault zone. The development of open joints and shear fractures at the edge of the indurated Jucurutu fault results in a fault-parallel zone of hydraulically conductive fracturing adjacent to the original, now indurated, fault damage zone with a lateral extent that exceeds 150 m. Thus the most hydraulically important part of the fault system is likely to be unaccounted for in current approaches to fault scaling and fracture modelling.

Our study demonstrates the importance of considering the geological history of an area, the previous deformation conditions and processes, and thus the mechanical and geometric attributes of the structures formed, as they exert a strong influence on the formation of later structures. We show that in basement terranes or settings that have experienced multiple deformation events, the complexity and longevity of the deformation history is an important consideration in developing accurate fracture and fault models for fluid flow prediction.

A.M.S., Z.K.S., R.J.L., S.I.P. and J.D.K. were supported by NERC grant NE/E005365/1. A.F.d.N. and F.H.R.B. were supported by INCT/CNPq Petroleum Geophysics, INCT/CNPq Tectonic Studies and CNPq grant 483349/2007-0. Thanks go to K. Dobson for her valuable assistance in the field.

References

Agosta, F., Alessandroni, M., Antonellini, M., Tondi, E. & Giorgioni, M. 2010. From fractures to flow: A field-based quantitative analysis of an outcropping carbonate reservoir. *Tectonophysics*, **490**, 197–213, http://dx.doi.org/10.1016/j.tecto.2010.05.005.

Aliverti, E., Biron, M., Francesconi, A., Mattiello, D., Nardon, S. & Peduzzi, C. 2003. Data analysis, processing and 3D fracture network simulation at wellbore scale for fractured reservoir description. *In*: Ameen, M. (ed.) *Fracture and In-Situ Stress Characterization of Hydrocarbon Reservoirs*. Geological Society, London, Special Publications, **209**, 27–37.

Arthaud, M.H., Caby, R., Fuck, R.A., Dantas, E.L. & Parente, C.V. 2008. Geology of the northern Borborema Province, NE Brazil and its correlation with Nigeria, NW Africa. *In*: Pankhurst, R.J., Trow, R.A.J., Brito Neves, B.B. & de Wit, M.J. (eds) *West Gondwana, Pre-Cenozoic Correlation across the South Atlantic Region*. Geological Society, London, Special Publications, **294**, 49–67.

Beacom, L.E., Holdsworth, R.E., McCaffrey, K.J.W. & Anderson, T.B. 2001. A quantitative study of the influence of pre-existing compositional and fabric heterogeneities upon fracture zone development during basement reactivation. *In*: Holdsworth, R.E., Strachan, R.A. & Magloughlin, J.F. (eds) *The Nature and Tectonic Significance of Fault Zone Weakening*. Geological Society, London, Special Publications, **186**, 195–211.

Belayneh, M.W., Matthai, S., Blunt, M.J.K. & Rogers, S.F. 2009. Comparison of deterministic with stochastic fracture models in water-flooding simulations. *AAPG Bulletin*, **93**, 1633–1648.

Brito Neves, B.B., Santos, E.J. & Van Schmus, W.R. 2000. Tectonic history of the Borborema Province, Northeastern Brazil. *In*: Cordani, U.G., Milani, E.J., Thomaz Filho, A. & Campos, D.A. (eds) *Tectonic Evolution of South America, 31st International Geological Congress*, *Rio de Janeiro*. 151–182.

Bruhn, R.L., Parry, W.T., Yonkee, W.A. & Thompson, T. 1994. Fracturing and hydrothermal alteration in normal fault zones. *Pure and Applied Geophysics*, **142**, 609–644.

Butler, R.W.H., Bond, C.E., Shipton, Z.K., Jones, R.R. & Casey, M. 2008. Fabric anisotropy controls faulting in the continental crust. *Journal of the Geological Society, London*, **165**, 449–452, http://dx.doi.org/10.1144/0016-76492007-129.

Caine, J.S., Evans, J.P. & Forster, C.B. 1996. Fault zone architecture and permeability structure. *Geology*, **24**, 1025–1028.

Chester, F.M. & Chester, J.S. 2000. Stress and deformation along wavy frictional faults. *Journal of Geophysical Research*, **105**, 23421–23430.

Chester, F.M., Chester, J.S., Kirschner, D.L., Schulz, S.E. & Evans, J.P. 2004. Structure of large-displacement, strike-slip fault zones in the brittle continental crust. *In*: Karner, G.D., Taylor, B., Driscoll, N.W. & Kohlstedt, (eds) *Rheology and Deformation in the Lithosphere at Continental Margins*. MARGINS Theoretical and Experimental Earth Science Series, Columbia University Press, New York, **1**, 223–260.

Childs, C., Manzocch, T., Walsh, J.J., Bonson, C.G., Nicol, A. & Schöpfer, M.P.J. 2009. A geometric model of fault zone and fault rock thickness variations. *Journal of Structural Geology*, **31**, 117–127.

Cooke, M.L., Simo, J.A., Underwood, C.A. & Rijken, P. 2006. Mechanical stratigraphic controls on fracture patterns within carbonates and implications for groundwater flow. *Sedimentary Geology*, **184**, 225–239.

Crider, J.G. & Peacock, C.P. 2004. Initiation of brittle faults in the upper crust: A review of field observations. *Journal of Structural Geology*, **26**, 691–707, http://dx.doi.org/10.1016/j.jsg.2003.07.007.

d'Alessio, M. & Martel, S.J. 2005. Development of strike-slip faults from dikes, Sequoia National Park, California. *Journal of Structural Geology*, **27**, 35–49.

Davatzes, N.C., Eichhubl, P. & Aydin, A. 2005. Structural evolution of fault zones in sandstone by multiple deformation mechanisms: Moab fault, southeast Utah. *Geological Society of America Bulletin*, **117**, 135–148, http://dx.doi.org/10.1130/B25473.1.

De Castro, D.L., Bezerra, F.H.R. & Branco, R.M.G.C. 2008. Geophysical evidence of crustal heterogeneity control of fault growth in the Neocomian Iguatu basin, NE Brazil. *Journal of South American Earth Sciences*, **26**, 271–285.

De Castro, D.L., Bezerra, F.H.R., Sousa, M.O.L. & Fuck, R.A. 2012. Influence of Neoproterozoic tectonic fabric on the origin of the Potiguar Basin, northeastern Brazil and its links with West Africa based on gravity and magnetic data. *Journal of Geodynamics*, **54**, 29–42, http://dx.doi.org/10.1016/j.jog.2011.09.002.

Downloaded from http://jgs.lyellcollection.org/ at University College Dublin on April 29, 2014

Degnan, P.J., Littleboy, A.K.McL., Lichie, U., Jackson, C.P. & Watson, S.P. 2003. Fracture-dominated flow in the Borrowdale Volcanic Group at Sellafield, NW England: The identification of potential flowing features, development of conceptual models and derivation of effective parameters. *In*: Petford, N. & McCaffrey, K.J.W. (eds) *Hydrocarbons in Crystalline Rocks*. Geological Society, London, Special Publications, **214**, 197–219.

Di Toro, G. & Pennacchioni, G. 2005. Fault plane processes and mesoscopic structure of a strong-type seismogenic fault in tonalites (Adamello batholith, Southern Italian Alps). *Tectonophysics*, **402**, 55–80.

Eichhubl, P., Davatzes, N.C. & Becker, S.P. 2009. Structural and diagenetic control of fluid migration and cementation along the Moab Fault, Utah. *AAPG Bulletin*, **93**, 653–681.

Evans, J.P., Forster, C.B. & Goddard, J.V. 1997. Permeability of fault-related rocks and implications for hydraulic structure of fault zones. *Journal of Structural Geology*, **19**, 1393–1404.

Fischer, M.P. & Polansky, A. 2006. The influence of flaws on joint spacing and saturation: Results of one-dimensional mechanical modelling. *Journal of Geophysical Research*, **111**, B07403, http://dx.doi.org/10.1029/2005JB004115.

Griffith, W.A., Mitchell, T.M., Renner, J. & Di Toro, G. 2012. Coseismic damage and softening of fault rocks at seismogenic depths. *Earth and Planetary Science Letters*, **353**, 219–230.

Guilbert, J.M. & Park, C.F. 1986. *The Geology of Ore Deposits*. Freeman, New York.

Henrikson, H. & Braathen, A. 2006. Effects of fracture lineaments and *in situ* stress on groundwater flow in hard rocks: A case study from Sunnfjord, western Norway. *Hydrogeological Journal*, **14**, 444–461.

Hesthammer, J. & Fossen, H. 2000. Uncertainties associated with fault sealing analysis. *Petroleum Geoscience*, **6**, 37–47.

Holdsworth, R.E., Stewart, M., Imber, J. & Strachan, R.A. 2001. The structure and rheological evolution of reactivated continental fault zones: A review and case study. *In*: Miller, J.A., Holdsworth, R.E., Buick, I.S. & Hand, M. (eds) *Continental Reactivation and Reworking*. Geological Society, London, Special Publications, **184**, 115–137.

Holford, S.P., Green, P.F., Hillis, R.R., Underhill, J.R., Stoker, M.S. & Duddy, I.R. 2010. Multiple post-Caledonian exhumation episodes across NW Scotland revealed by apatite fission-track analysis. *Journal of the Geological Society, London*, **167**, 675–694, http://dx.doi.org/10.1144/0016-76492009-167.

Johansen, T.E.S., Fossen, H. & Kluge, R. 2005. The impact of syn-faulting porosity reduction on damage zone architecture in porous sandstone: An outcrop example from the Moab Fault, Utah. *Journal of Structural Geology*, **27**, 1469–1485.

Jolley, S.J., Dijk, H., Lamens, J.H., Fisher, Q.J., Manzocchi, T., Eikmans, H. & Huang, Y. 2007. Faulting and fault sealing in production simulation models: Brent Province, northern North Sea. *Petroleum Geoscience*, **13**, 321–340.

Kirkpatrick, J.D., Bezerra, F.H.R., Shipton, Z.K., do Nascimento, A.F., Pytharouli, S.I., Lunn, R.J. & Soden, A.M. 2013. Scale-dependent influence of pre-existing basement shear zones on rift faulting: A case study from northeast Brazil. *Journal of the Geological Society, London*, **170**, 237–247.

Koning, T. 2003. Oil and gas production from basement reservoirs: Examples from Indonesia, USA and Venezuela. *In*: Petford, N. & McCaffrey, K.J.W. (eds) *Hydrocarbons in Crystalline Rocks*. Geological Society, London, Special Publications, **214**, 83–92.

Laubach, S.E., Olson, J.E. & Gross, M.R. 2009. Mechanical and fracture stratigraphy. *AAPG Bulletin*, **93**, 1413–1426.

Le Garzic, E., de L'Hamaide, T., *et al.* 2011. Scaling and geometric properties of extensional fracture systems in the Proterozoic basement of Yemen. Tectonic interpretation and fluid flow implications. *Journal of Structural Geology*, **33**, 519–536.

Lisker, F. 2004. The evolution of the geothermal gradient from Lambert Graben and Mahanadi Basin—a contribution to the Indo-Antarctic rift debate. *Gondwana Research*, **7**, 363–373.

Manzocchi, T., Childs, C. & Walsh, J.J. 2010. Fault and fault properties in hydrocarbon flow models. *Geofluids*, **10**, 94–113.

Matos, R.M.D. 1992. The northeast Brazilian rift system. *Tectonics*, **11**, 766–791.

Mauldon, M., Dunne, W.M. & Rohrbaugh, M.B., Jr. 2001. Circular scanlines and circular windows: New tools for characterizing the geometry of fracture traces. *Journal of Structural Geology*, **23**, 247–258.

McConaughy, D.T. & Engelder, T. 2001. Joint initiation in bedded clastic rocks. *Journal of Structural Geology*, **23**, 203–221.

Moir, H., Lunn, R.J., Shipton, Z.K. & Kirkpatrick, J.D. 2010. Simulating brittle fault evolution from networks of pre-existing joints within crystalline rock. *Journal of Structural Geology*, **32**, 1742–1753, http://dx.doi.org/10.1016/j.jsg.2009.08.016.

Moir, H., Lunn, R.J., Micklethwaite, S. & Shipton, Z.K. 2013. Distant off-fault damage and gold mineralization: The impact of rock heterogeneity. *Tectonophysics*, **608**, 461–446, http://dx.doi.org/10.1016/j.tecto.2013.08.043.

Morais Neto, J.M., Hegarty, K.A., Karner, G.D. & Alkmim 2009. Timing and mechanisms for the generation and modification of the anomalous topography of the Borborema Province, northeastern Brazil. *Marine and Petroleum Geology*, **26**, 1070–1086, http://dx.doi.org/10.1016/j.marpetgeo.2008.07.002.

Mitchell, T.M. & Faulkner, D.R. 2012. Towards quantifying the matrix permeability of fault damage zones in low porosity rock. *Earth and Planetary Science Letters*, **339–349**, 24–31.

Myers, R.D., Allgood, A., Hjellbakk, A., Vrolijk, P. & Briedis, N. 2007. Testing fault transmissibility predictions in a structurally dominated reservoir: Ringhorne Field, Norway. *In*: Jolley, S.J., Barr, D., Walsh, J.J. & Knipe, R.J. (eds) *Structurally Complex Reservoirs*. Geological Society, London, Special Publications, **292**, 271–294.

Nóbrega, M.A., Sá, J.M., *et al.* 2005. The use of apatite fission track thermochronology to constrain fault movements and sedimentary basin evolution in northeastern Brazil. *Radiation Measurements*, **39**, 627–633.

Pollard, D.D. & Aydin, A.A. 1988. Progress in understanding jointing over the past century. *Geological Society of American Bulletin*, **100**, 1181–1204.

Pytharouli, S.I., Lunn, R.J., Shipton, Z.K., Kirkpatrick, J. & do Nascimento, A.F.D. 2011. Microseismicity illuminates fluid pathways in the shallow crust. *Geophysical Research Letters*, **38**, L02402, http://dx.doi.org/10.1029/2010GL045875.

Sanders, C.A.E., Fullarton, L. & Calvert, S. 2003. Modelling fracture systems in extensional crystalline basement. *In*: Petford, N. & McCaffrey, K.J.W. (eds) *Hydrocarbons in Crystalline Rock*. Geological Society, London, Special Publications, **214**, 7–33.

Sausse, J., Fourar, M. & Genter, A. 2006. Permeability and alteration within the Soultz granite inferred from geophysical and flow log analysis. *Geothermics*, **35**, 544–560, http://dx.doi.org/10.1016/j.geothermics.2006.07.003.

Savage, H.M. & Brodsky, E.E. 2011. Collateral damage: Evolution with displacement of fracture distribution and secondary fault strands in fault damage zones. *Journal of Geophysical Research*, **116**, B03405, http://dx.doi.org/10.1029/2010JB007665.

Schultz, S.E. & Evans, J.P. 1998. Spatial variability in microscopic deformation and composition of the Punchbowl fault, southern California: Implications for mechanisms, fluid–rock interaction, and fault morphology. *Tectonophysics*, **295**, 223–244.

Schutter, R.S. 2003. Hydrocarbon occurrence and exploration in and around igneous rocks. *In*: Petford, N. & McCaffrey, K.J.W. (eds) *Hydrocarbons in Crystalline Rocks*. Geological Society, London, Special Publications, **214**, 7–33.

Shackleton, J.R., Cooke, M.L. & Sussman, A.J. 2005. Evidence of temporally changing mechanical stratigraphy and effects on joint-network architecture. *Geology*, **33**, 101–104.

Shea, W.T. & Kronenberg, A.K. 1993. Strength anisotropy of foliated rocks with varied mica contents. *Journal of Structural Geology*, **15**, 1097–1121.

Shipton, Z.K., Soden, A.M., Kirkpatrick, J.D., Bright, A.M. & Lunn, R.J. 2006. How thick is a fault? Fault displacement–thickness scaling revisited. *In*: Abercrombie, R., McGarr, A., di Toro, G. & Kanamori, H. (eds) *Earthquakes: Radiated Energy and the Physics of Faulting*. Geophysical Monograph, American Geophysical Union, **170**, 193–198.

Sibson, R.H. & Toy, V.G. 2006. The habitat of fault-generated pseudotachylyte: Presence vs. absence of friction-melt. *In*: Abercrombie, R., McGarr, A., di Toro, G. & Kanamori, H. (eds) *Earthquakes: Radiated Energy and the Physics of Faulting*. Geophysical Monograph, American Geophysical Union, **170**, 153–166.

Sleight, J.M., McCaffrey, K.J.W. & Holdsworth, R.E. 2001. Micro to regional scale fracture characteristics from the More Trondelag Fault Complex, Central Norway. *In*: *Hydrocarbons in Crystalline Rocks*, *Abstracts Book*. London.

Slightam, C. 2012. Characterizing seismic-scale faults pre- and post-drilling; Lewisian Basement, West of Shetlands. *In*: Spence, G.H., Redfern, J., Aguilera, R., Bevan, T.G., Cosgrove, J.W., Couples, G.D. & Daniel, J.-M. (eds) *Advances in the Study of Fractured Reservoirs*. Geological Society, London, Special Publications, **374**, http://dx.doi.org/10.1144/SP374.6.

Soden, A.M. & Shipton, Z.K. 2013. Dilational fault zone architecture in a welded ignimbrite: The importance of mechanical stratigraphy. *Journal of Structural Geology*, **51**, 156–166, http://dx.doi.org/10.1016/j.jsg.2013.02.001.

Tenthorey, E. & Cox, S.F. 2006. Cohesive strengthening of fault zones during the interseismic period: An experimental study. *Journal of Geophysical Research*, **111**, http://dx.doi.org/10.1029/2005JB004122.

Tenthorey, E. & Fitz Gerald, J.D. 2006. Feedback between deformation, hydrothermal reaction and permeability evolution in the crust: Experimental insights. *Earth and Planetary Science Letters*, **247**, 117–129.

Downloaded from http://jgs.lyellcollection.org/ at University College Dublin on April 29, 2014

TIEN, Y.M., KUO, M.C. & JUANG, C.H. 2006. An experimental investigation of the failure mechanism of simulated traversely isotropic rocks. *International Journal of Rock Mechanics and Mining Sciences*, **43**, 1163–1181.

TORABI, A. & BERG, S.S. 2011. Scaling of fault attributes: A review. *Marine and Petroleum Geology*, **28**, 1444–1460.

VAUCHEZ, A., PACHECO-NEVES, S., CABY, R., CORSINI, M., EGYDIO-SILVA, M., ARTHAUD, M. & AMARO, V. 1995. The Borborema shear zone system. *Journal of South American Earth Sciences*, **8**, 247–266.

WILSON, J.E., GOODWIN, L.B. & LEWIS, C.J. 2003. Deformation bands in nonwelded ignimbrites: Petrophysical controls on fault-zone deformation and evidence of preferential fluid flow. *Geology*, **31**, 837–840.

YIELDING, G., FREEMAN, B. & NEEDHAM, D.T. 1997. Quantitative fault seal prediction. *AAPG Bulletin*, **81**, 897–917.

YOUNES, A.I., ENGELDER, T. & BOSWORTH, W. 1998. Fracture distribution in faulted basement blocks: Gulf of Suez, Egypt. *In*: COWARD, M.P., DALTABAN, T.S. & JOHNSON, H. (eds) *Structural Geology in Reservoir Characterization*. Geological Society, London, Special Publications, **127**, 167–190.

Received 2 May 2013; revised typescript accepted 3 February 2014.
Scientific editing by Ian Alsop.